EC Journals.ASM.org

N-Acetylglucosamine (GlcNAc)-Inducible Gene *GIG2* Is a Novel Component of GlcNAc Metabolism in *Candida albicans*

Swagata Ghosh,[a] Kongara Hanumantha Rao,[a] Neel Sarovar Bhavesh,[b] Gobardhan Das,[c] Ved Prakash Dwivedi,[c] Asis Datta[a]

National Institute of Plant Genome Research, New Delhi, India[a]; Structural and Computational Biology Group, International Centre for Genetic Engineering and Biotechnology (ICGEB), New Delhi, India[b]; Immunology Group, International Centre for Genetic Engineering and Biotechnology (ICGEB), New Delhi, India[c]

Candida albicans **is an opportunistic fungal pathogen that resides in the human body as a commensal and can turn pathogenic when the host is immunocompromised. Adaptation of *C. albicans* to host niche-specific conditions is important for the establishment of pathogenicity, where the ability of *C. albicans* to utilize multiple carbon sources provides additional flexibility. One alternative sugar is *N*-acetylglucosamine (GlcNAc), which is now established as an important carbon source for many pathogens and can also act as a signaling molecule. Although GlcNAc catabolism has been well studied in many pathogens, the importance of several enzymes involved in the formation of metabolic intermediates still remains elusive. In this context, microarray analysis was carried out to investigate the transcriptional responses induced by GlcNAc under different conditions. A novel gene that was highly upregulated immediately following the GlcNAc catabolic genes was identified and was named *GIG2* (GlcNAc-induced gene 2). This gene is regulated in a manner distinct from that of the GlcNAc-induced genes described previously in that GlcNAc metabolism is essential for its induction. Furthermore, this gene is involved in the metabolism of *N*-acetylneuraminate (sialic acid), a molecule equally important for initial host-pathogen recognition. Mutant cells showed a considerable decrease in fungal burden in mouse kidneys and were hypersensitive to oxidative stress conditions. Since *GIG2* is also present in many other fungal and enterobacterial genomes, targeted inhibition of its activity would offer insight into the treatment of candidiasis and other fungal or enterobacterial infections.**

The opportunistic fungal pathogen *Candida albicans* colonizes numerous niches within the human host (1–3) and causes infections at mucosal surfaces in the oral cavity and in the gastrointestinal and urogenital tracts. During their adaptation to changing microenvironments, pathogens also encounter the added challenge of contending with host defenses (4).

For this purpose, *C. albicans* has evolved specific counterdefense strategies, the molecular mechanisms of which are poorly understood. *C. albicans* regularly colonizes glucose-poor niches in the host and thus depends on alternative carbon sources for its growth (5). *N*-Acetylglucosamine (GlcNAc) is one such sugar whose metabolism and linkage with other pathways central to carbon assimilation or morphopathogenic signaling (6–8) remains understudied, although its utilization pathway is conserved from pathogenic bacteria to eukaryotes (9).

The enzymes needed to catabolize GlcNAc include Ngt1 (a transporter that takes up GlcNAc), Hxk1 (a kinase that converts GlcNAc to GlcNAc-6-phosphate), Dac1 (a deacetylase that converts GlcNAc-6-phosphate to glucosamine-6-phosphate), and Nag1 (a deaminase that converts glucosamine-6-phosphate to glucose-6-phosphate) (10–13). For organisms in which GlcNAc utilization seems to be quite common, the steps involved in the bifurcation or metabolism (other than the GlcNAc catabolic pathway) of GlcNAc-6-phosphate, once it is formed, are poorly characterized (14). Our present study, which deals with a gene upregulated in deacetylase and deaminase mutants of *C. albicans*, sheds some light on this understudied route emanating from *N*-acetylglucosamine-6-phosphate, which appears to be a central molecule for several anabolic and catabolic processes (9, 15). The new GlcNAc-induced gene *GIG2*, a DUF1479 family member, has not been characterized in any organism previously. We characterize this gene in *C. albicans* by using multiple experimental approaches. The *GIG2* mutant was sensitive to H_2O_2 and showed reduced virulence in a murine model. Affinity purification of the protein followed by mass spectrometry led to the identification of *N*-acetylneuraminate as its substrate. We therefore report that the *GIG2* gene is present in the route where *N*-acetylneuraminic acid (Neu5Ac, or NANA) is formed from *N*-acetylglucosamine-6-phosphate.

This study thus focuses on an uncharacterized cross talk between a stress-adaptive mechanism and GlcNAc utilization, and Gig2 is added to the ever-growing list of virulence factors that probably contribute to the early events of *C. albicans* infection. Though preliminary, our results delineate the pathway where this GlcNAc-inducible gene, which is well conserved in several enterobacterial and fungal pathogens, works; however, the catalytic reaction of Gig2 for the production of Neu5Ac and the exact role of this pathway in the attenuation of virulence still remain elusive.

MATERIALS AND METHODS

Media and growth conditions. The standard media YPD (yeast extract-peptone-dextrose) and SD (synthetic dextrose) (16) were used routinely for strain growth and maintenance. SN plates were supplemented with GlcNAc instead of glucose. Selection for *URA3* prototrophy and counterselection against *URA3* were performed as described previously (17). Spider medium at 37°C (16), 2.5 mM GlcNAc in a salt base containing 0.45%

Received 12 September 2013 **Accepted** 22 October 2013
Published ahead of print 1 November 2013
Address correspondence to Asis Datta, asis_datta@rediffmail.com.
S.G. and K.H.R. contributed equally to this article.
Supplemental material for this article may be found at http://dx.doi.org/10.1128/EC.00244-13.

doi:10.1128/EC.00244-13

NaCl, and 0.335% YNB (yeast nitrogen base) without amino acids at 37°C (18) were used both for colony growth assays and for the induction of filamentation.

For induction on Spider medium plates, the cells were counted, plated at a concentration of 40 to 50 cells per plate, and incubated for 5 days at 30°C. For YPD and GlcNAc media, cells were plated similarly and were incubated at 37°C and 30°C, respectively, for 5 days. Sensitivity to nikkomycin Z, Congo red, and calcofluor white was tested by spotting dilutions of cells onto YPD plates (or onto SD or SN plates for nikkomycin Z) fortified with the respective chemical. In order to determine the effect of H_2O_2, cells were grown in YPD broth for 1 h; H_2O_2 was added at the required concentrations (5 and 10 mM); and dilution series were then spotted onto YPD plates without H_2O_2.

DNA manipulations. (i) Preparation of the *gig2* mutant. The *GIG2* (ORF19.4783) deletion mutant was constructed in *C. albicans* strain SN152 using the method described previously (19, 20). Precisely, PCR primers (GIG2-DEL-F and GIG2-DEL-R) were used to amplify either the *LEU2* or the *HIS1* selectable marker gene (from plasmid pSN40 or pSN52, respectively). The integration of the deletion cassettes at the appropriate sites was verified by performing PCR using combinations of primers that flanked the integration sites as well as primers that annealed within the integrated cassettes (CHECK-MUT1, CHECK-LEU2, and CHECK-HIS1). Complemented strains were constructed by transforming a plasmid carrying one wild-type (WT) copy of *C. albicans GIG2* (*CaGIG2*) and the *ARG4* selectable marker gene into the *C. albicans* genome (primer CHECK-ARG4 was used for confirmation). The primers and strains used in this study are listed in Tables S1 and S2 in the supplemental material, respectively.

(ii) Epitope and GFP tagging. PCR was performed by using plasmid pGFP-URA3 (21) as the template and appropriate gene-specific primers, namely, GIG2-GP-F1 and GIG2-UR-R1. The PCR product was used for the transformation of a *C. albicans* Ura$^-$ strain, CAI4. Transformations were identified by PCRs using one primer that annealed within the transformation module (Tag1) and a second primer that annealed to the target gene locus outside the altered region (Tag2). The same strain (iGIG2-GFP) was reconfirmed by Western blot analysis using an antibody against green fluorescent protein (GFP). Myc-tagged (iHXK1-Myc and iNGT1-Myc) and hemagglutinin (HA)-tagged (iGIG2-HA) strains were prepared as described above by using pFA5a-13Myc.URA3 and pFA5a-3HA.URA3 (22), respectively, as the templates.

(iii) TAP tagging. To tandemly tag CaGig2p with the HF (6×His and Flag) epitope in the genomic locus, a DNA fragment containing the 3′ region of *GIG2*, the 6×HF tag sequence, the *ACT1* terminator, the *URA3* marker, and the downstream region of *GIG2* was amplified by using p6HF-ACT1 (23) as the template and GIG2-HFL-F and GIG2-UR-R1 as primers, and the amplification product was introduced into CAI4 to generate iGIG2-HF.

Western blotting. Protein extracts were prepared from *C. albicans* cells and were subjected to Western blot analysis as described previously (24). For detection of the proteins tagged with the HA epitope, membranes were incubated with an anti-HA monoclonal antibody (Roche) at a dilution of 1:1,000 and a peroxidase-conjugated secondary antibody (Amersham Biosciences, United Kingdom) at a dilution of 1:20,000. For detection with an anti-FLAG antibody (Sigma), the dilution was 1:4,000 in 3% skim milk (Difco) in Tris-buffered saline with 0.05% Tween 20 (TBST).

Quantitative real-time PCR. For all reverse-transcription-PCR (RT-PCR) experiments, total RNA isolated using TriPure isolation reagent was treated with RNase-free DNase I (Invitrogen) to remove any residual DNA. About 500 ng of this RNA was used for single-stranded cDNA synthesis by using a High-Capacity cDNA reverse transcription kit (Applied Biosystems), and the cDNA was used for quantitative RT-PCR (qRT-PCR) with SYBR green PCR master mix on an ABI Prism 7000 real-time PCR apparatus (Applied Biosystems). The comparative threshold cycle (C_T) method ($2^{-\Delta\Delta CT}$) was used to determine relative gene expression (25). Control reactions without reverse transcriptase were carried out for each cDNA preparation and ascertained that no amplification was obtained, as judged by high C_T values and gel analysis.

Isolation of peritoneal macrophages and fluorescence assay. Mice (BALB/c) were injected intraperitoneally with 2 ml of 4% thioglycolate (Brewer Modified; BBL; Becton Dickinson [BD], USA). Five days later, peritoneal exudates were isolated from the peritoneal cavity by washing with ice-cold RPMI 1640 medium supplemented with 10% fetal bovine serum (FBS; Thermo Scientific HyClone, USA). Cells were cultured overnight at 37°C under 5% CO_2 and were washed with RPMI medium–10% FBS to remove nonadherent cells. Adherent monolayer cells were used as peritoneal macrophages. Peritoneal macrophages (1×10^5 ml^{-1}) were cultured in RPMI medium and were infected with wild-type *C. albicans* and *C. albicans* mutants at a multiplicity of infection (MOI) of 1:1 for 45 min. Then the cells were washed with fresh RPMI medium twice; fresh RPMI medium was added to the cells; and the cells were cultured at 37°C under 5% CO_2 for 1 h.

Fluorescence-activated cell sorter (FACS) analysis. For fluorescence, the cells were washed twice with phosphate-buffered saline (PBS) and were resuspended in PBS for data acquisition. Fluorescence intensity was measured by flow cytometry (FACSCanto II; BD), and the data were analyzed with FlowJo (TreeStar, USA).

Mouse infection studies. Animal experiments (with BALB/c mice, 6 to 8 weeks of age) were performed according to the guidelines approved by the Institutional Animals Ethics Committee of Jawaharlal Nehru University. Control mice were injected with 100 μl PBS as a vehicle control. Cohorts of 5 mice per *C. albicans* strain were inoculated for a survival study. For infection, one colony from each *C. albicans* strain was inoculated into 50 ml of YPD medium. Cultures were grown overnight, washed twice with 50 ml of sterile water, counted by hemocytometry, and resuspended at 10^7 cells ml^{-1} in sterile water. Eight- to 9-week-old mice were injected with 0.3 ml (3×10^6 cells) of culture or with PBS via the lateral tail vein, and the course of infection was monitored for as long as 18 days. Infected mice were considered moribund when they could no longer reach food or water. Moribund mice, as well as mice surviving to the end of the experiment, were euthanized by anesthetization followed by cervical dislocation. In order to assess the fungal burden in kidney tissue, the dose described above was injected (5 mice per strain per experiment), and mice were sacrificed at varying time points (24, 42, and 72 h) postinfection. Kidneys from individual mice (3 to 5 mice per group) were removed aseptically, weighed, and homogenized in 1× PBS buffer by using a homogenizer. CFU counts were determined by plating serial dilutions on YPD agar medium. The colonies were counted after 24 h at 37°C, and results were expressed as log CFU per gram of tissue. These experiments were performed three times with 3 to 5 mice per group. For histopathological studies, kidneys removed 72 h postinfection were fixed in 10% formaldehyde–PBS, sectioned in paraffin blocks, and stained with periodic acid-Schiff reagent and hematoxylin-eosin (H&E) stain. Examination was performed under a light microscope, and photographs were taken with a Nikon camera fitted to the microscope.

Affinity purification and metabolite extraction. Frozen yeast cell pellets from 500-ml cultures were resuspended in 5 ml lysis solution (200 mM ammonium acetate, 1× Complete protease inhibitor cocktail [Roche], and 1 mM EGTA). One volume of glass beads (Sigma) was added to facilitate cell lysis by vortexing for 15 cycles (1 min of vortexing and 1 min of resting on ice), followed by centrifugation at 13,400 × *g* for 30 min. The supernatants were then subjected to TAP as described by Rao et al. in 2013 (26) with some modifications. In the first round of purification, cell lysates were incubated with 50 ml of anti-FLAG M2 agarose (Sigma) for 2 h at 4°C, and a second round of purification was performed with Ni-nitrilotriacetic acid (NTA) agarose (Qiagen) for 1 h at 4°C. The beads were washed once for 5 min in 300 mM ammonium acetate and once for 5 min in 150 mM ammonium acetate. To extract the protein-bound metabolites (27), 60 ml of pure methanol was added to the beads twice, and the beads were incubated at room temperature for 10 min. The methanol

extract was then immediately transferred to a Waters Max Recovery glass vial and was analyzed by mass spectrometry. The beads were then boiled in 50 ml of 1× SDS sample buffer for 5 min, and 15 ml of the supernatant was resolved on a 12% SDS-PAGE gel, followed by a silver staining reagent (Bio-Rad).

UPLC-coupled ESI mass spectrometry. The mass spectrometry system used in this study comprised an Acquity ultraperformance liquid chromatograph (UPLC) system and a Synapt G2 mass spectrometer equipped with an electrospray ionization (ESI) probe (Waters Co., Milford, MA). For each run, 10 μl metabolite extract was loaded onto a C_{18} column using a binary solvent gradient of 5% to 95% methanol in water for 12 min and 95% methanol for another 5 min. The collection mass range was 100 to 1,200 *m/z* in profile scan mode to avoid missing uncommon mass adducts. The probe and source temperatures were 500°C and 130°C, respectively. The data were processed though MarkerLynx software, version 4.1 (Waters Co., Milford, MA) (27).

NMR spectroscopy. Wild-type and *gig2* and *dac1* (14) mutant strains were selected for nuclear magnetic resonance (NMR) analysis of metabolites. Exponentially grown cells in SD medium were collected, washed twice, and induced in SN medium (with a stable isotope of *N*-acetyl-D-[1-^{13}C]glucosamine) for 2 h. The metabolites were extracted as described by Yu et al. in 2013 (28). The dried sample was dissolved in 200 μl D_2O and was used for measuring NMR spectra.

Two-dimensional (2D) ^{13}C,^{1}H heteronuclear single quantum coherence (HSQC) spectra were measured at 25°C on a Bruker Avance III spectrometer equipped with a cryogenic triple-resonance TCI probe head, operating at a field strength of 500 MHz. Temperature calibration was performed using a 100% d_4-methanol sample (29). All spectra were acquired and processed with TopSpin, version 2.1 (Bruker AG). All data were analyzed using CARA (30). Standard 2D ^{13}C,^{1}H HSQC spectra and peak lists deposited in the Biological Magnetic Resonance Data Bank (BMRB) (http://www.bmrb.wisc.edu/; accession no. bmse000231, bmse000163, bmse000205, and bmse000057) and the Human Metabolome Database (HDMB) (http://www.hmdb.ca/; HMDB identification no. HMDB00290, HMDB00803, and HMDB00230) were used for the identification of resonance peaks.

RESULTS

***GIG2* induction is specific to GlcNAc.** Comparative microarray analysis of glucose versus GlcNAc and of glycerol versus GlcNAc showed ORF19.4783 to be a prominently induced gene; the level of induction was ~28-fold for GlcNAc versus glucose and ~22-fold for GlcNAc versus glycerol. Interestingly, this gene showed downregulation in an *hxk1* mutant in response to GlcNAc (Fig. 1A). Western blot analysis with a strain in which this gene was C-terminally tagged with a 3×HA tag revealed that its expression is specific only for GlcNAc and not for other sugars, such as *N*-acetylmannosamine (ManNAc), *N*-acetylgalactosamine (GalNAc), galactose, and glucose, or for nonfermentable carbon sources, such as glycerol, lactate, acetate, citrate, and ethanol (Fig. 1B).

ORF19.4783 turned out to be a conserved hypothetical protein of 474 amino acids and a member of the DUF1479 family. We named it *GIG2* (GlcNAc-induced gene) in accordance with the name *GIG1* reported by Gunasekera et al. in 2010 (31). For protein localization data, we chromosomally tagged *GIG2* at the C-terminal region with a GFP sequence (21). The Gig2-GFP fusion protein localized to the cytoplasm in the presence of 2% GlcNAc (Fig. 1C). This further confirmed that this gene is induced by GlcNAc and that the corresponding functional protein is one of the proteins linked to GlcNAc metabolism. Our study provides the first evidence that at least one member of the DUF1479 family shows protein expression specific to GlcNAc and localizes in the cytoplasm. Strains iGIG2-GFP and iGIG2-HA were checked for functionality by their abilities to complement the growth defects shown by the *gig2* mutant strain in the presence of H_2O_2 (see Fig. S1 in the supplemental material).

GlcNAc catabolism is required for GlcNAc-specific induction of *GIG2*. Previous studies (14, 26) have indicated that GlcNAc directly induces GlcNAc catabolic gene expression irrespective of GlcNAc catabolism. In addition to direct induction by GlcNAc, metabolic intermediates arising out of catabolism can also regulate gene expression in the overall process of GlcNAc metabolism. These facts were clear from expression analysis of an *hxk1* mutant compared with the wild type in response to GlcNAc (Fig. 1A; see also Fig. S2 in the supplemental material). Further, we carried out real-time RT-PCR analysis in order to understand the expression patterns of *GIG2* and other GlcNAc-inducible genes in wild-type *C. albicans* and catabolic pathway mutants in the presence of GlcNAc. Surprisingly, *GIG2* was downregulated 12-fold in the *hxk1* mutant, whereas *NAG1* and *GAL10* expression levels were unaltered (Fig. 1A and D). Then we checked for the expression of *GIG2* in the *dac1*and *nag1* mutant backgrounds and found the gene to be upregulated at least 2-fold compared to expression in GlcNAc-grown wild-type cells (Fig. 1D). We hypothesized that the downregulation of *GIG2* in the *hxk1* mutant could be due to the inability of the *hxk1* mutant to form GlcNAc-6-phosphate. Otherwise stated, GlcNAc catabolism or, more specifically, GlcNAc-6-phosphate, an intermediary product of GlcNAc catabolism, seemed to be essential for the induction of this gene. Thus, Gig2 probably acts at a point downstream of Hxk1 and upstream of Dac1 and Nag1, at a place where GlcNAc-6-phosphate diverges to other anabolic pathways. This interesting observation provided clues for understanding the poorly studied biochemical pathways in *C. albicans* emanating from GlcNAc-6-phosphate, which are probably conserved among pathogenic fungi and enterobacterial species.

Gig2 protein is induced late. Western blot analysis was performed for protein extracts obtained from cells (iGIG2-HA) induced and collected at different time points. Gig2 was detectable at least after 30 min of induction and reached peak levels at 120 to 180 min of induction (Fig. 1E, top), whereas the GlcNAc catabolic enzymes Ngt1 and Hxk1 reached maximum levels within 30 and 60 min of induction, respectively (Fig. 1E, bottom) (10). This late induction of Gig2 could be due to a secondary response of the cell to GlcNAc, where a probable increase in the pool of GlcNAc-6-phosphate initiates other pathways (of which Gig2 may be a member) diverging from this intermediary metabolite. The probable significance of late induction is discussed below.

The *gig2* mutant exhibited reduced filamentation under some inducing conditions and showed uncompromised growth on GlcNAc. Since dimorphism is a long-suspected mechanism of virulence (13, 32), we investigated the effect of disruption of *GIG2* on the colony morphology of *C. albicans* on plates containing established media such as YPD (37°C), Spider, and GlcNAc media. Hyphal formation by homozygous mutants was impaired to some extent under all of the conditions mentioned above, and these mutants were mostly smooth at the periphery (Fig. 2A). Interestingly, after 5 days, 35% of colonies in YPD medium at 37°C showed a sectored morphology with distinct white and opaque regions; the reasons for this phenomenon are not known. The ability of the *gig2* mutant strain to grow on GlcNAc was also checked by spotting serial dilutions of cells onto a solid agar me-

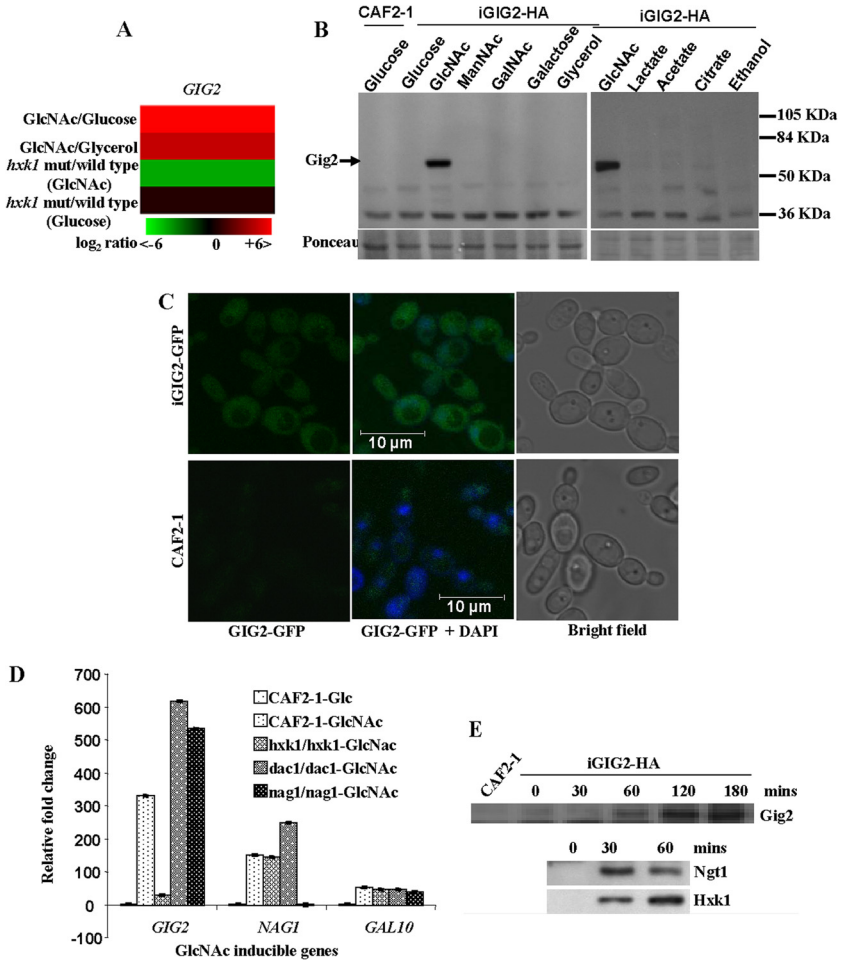

FIG 1 GlcNAc-specific expression of *GIG2*. (A) Heat map showing the ratio of differential expression of *GIG2* in response to GlcNAc under four different conditions. The average expression values obtained from two biological replicates with dye swap were used. The color scale at the bottom indicates the $\log_2$ ratio. (B) Gig2-HA is specifically induced by GlcNAc. The untagged control strain CAF2-1 or the HA-tagged strain iGIG2-HA was grown in a synthetic medium containing the indicated sugars (2% each) for 3 h. Western blotting was performed with an anti-HA antibody. Ponceau-stained bands are shown as a loading control. (C) Gig2 localizes to the cytoplasm. The wild-type untagged control strain CAF2-1 or the GIG2-GFP strain iGIG2-GFP was grown in a synthetic medium containing 2% GlcNAc for 3 h and was visualized by confocal microscopy. The central panel shows a merged view of cells under GFP and 4′,6-diamidino-2-phenylindole (DAPI) filters. (D) Relative expression of GlcNAc-inducible gene transcripts in wild-type *C. albicans* (CAF2-1) and in GlcNAc catabolic pathway mutants (*hxk1*, *dac1*, and *nag1* mutants). *ACT1* (encoding actin) was used as the endogenous control. All experiments were performed with two biological replicates; each sample was loaded in triplicate for qPCR. Error bars represent coefficients of variation. (E) Time kinetics for the expression of Gig2 protein and of the GlcNAc catabolic proteins Ngt1 and Hxk1. Shown is the expression of Gig2 (top), Ngt1, and Hxk1 (bottom) after the addition of GlcNAc. Cell extracts from different strains at different time points (as indicated) were analyzed by Western blotting and were probed with an anti-HA or anti-c-Myc antibody.

dium containing either GlcNAc or dextrose as the carbon source. No difference in the growth rate was observed (Fig. 2B). Thus, *GIG2* is not needed for normal growth on GlcNAc plates but contributes to some extent toward filament formation under hypha-inducing conditions.

The *gig2* mutant showed sensitivity to hydrogen peroxide. Our results show that *GIG2* is not involved in the main GlcNAc catabolic cascade and is induced late upon GlcNAc addition. We presumed this gene to be a member of the secondary metabolic pathways arising out of GlcNAc-6-phosphate that could be instrumental in combating stress responses. Therefore, we checked the sensitivities of the mutant and wild-type strains to a range of stress-inducing agents. Notably, deletion of *GIG2* specifically resulted in impaired resistance to the oxidative-stress-inducing agent H_2O_2 (Fig. 2C) at low concentrations (5 and 10 mM). In contrast, no notable increase in sensitivity to other oxidative-stress-inducing agents, such as Na_3N (an inhibitor of complex III), or to cell wall biogenesis inhibitors, such as calcofluor white and Congo red, was observed. Similarly, no marked difference could be observed in the mutants when they were grown in the presence of the chitin synthase inhibitor nikkomycin Z (Fig. 2D).

Gig2-GFP is induced by macrophage phagocytosis. Previous reports have shown that *C. albicans* has evolved mechanisms to induce the utilization of carbon sources other than glucose upon engulfment by macrophages, probably to facilitate the utilization of host-derived macromolecules, and, furthermore, that the interaction of *C. albicans* with macrophages is considered a crucial step in the development of an adequate immune response in systemic candidiasis (33). Interestingly, Gig2-GFP was induced after phagocytosis by primary murine macrophages in three indepen-

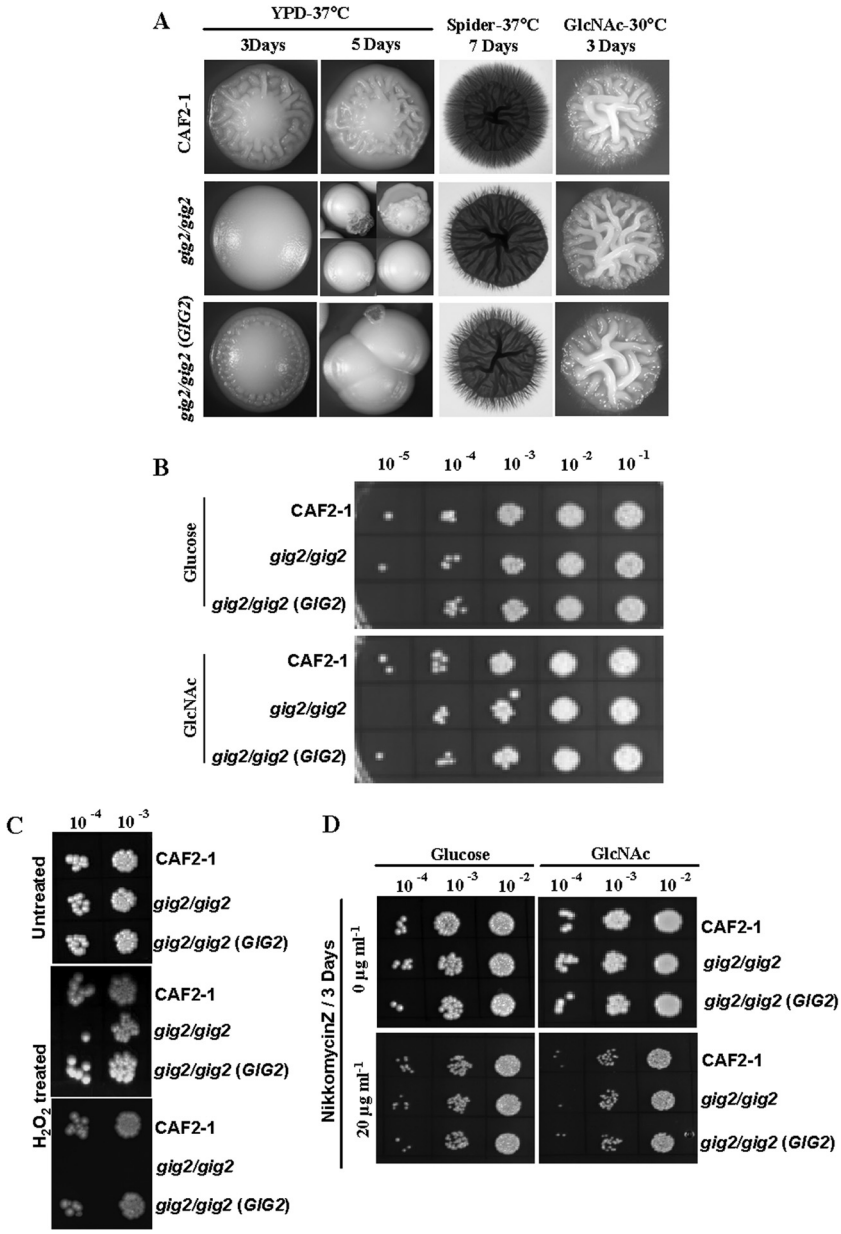

FIG 2 Morphogenesis and growth analysis of *gig2* mutant cells. (A) The *gig2* mutant showed reduced filamentation on YPD and Spider media (37°C) and on SN medium (30°C) under the conditions indicated. (B) The *gig2* mutant showed unaltered growth on GlcNAc plates. Tenfold dilution series of the indicated *C. albicans* strains were spotted onto synthetic medium agar plates containing either glucose or GlcNAc at 2%. (C) Response of the *gig2* mutant to hydrogen peroxide. For H_2O_2 stress, wild-type, *gig2* mutant, and revertant strains were grown and either left untreated (top) or treated with 5 mM (center) or 10 mM (bottom) H_2O_2. The untreated and treated cells were spotted onto YPD plates and were incubated at 30°C for 2 days. (D) Response of the *gig2* mutant to nikkomycin Z. Strains were grown in YPD medium for 8 h at 30°C, and 10-fold dilution series were spotted onto plates containing either SD medium alone, SD medium plus nikkomycin Z (20 μg ml^{-1}), or SN medium plus nikkomycin Z (20 μg ml^{-1}).

dent experiments, and there was some nonspecific fluorescence in macrophages that had phagocytosed untagged wild-type cells. The level of Gig2-GFP was readily detected above this background. FACS analysis with the iGIG2-GFP strain (5-fold increase in expression over that of untagged infected cells) also supported the epifluorescence observation (see Fig. S3A and B in the supplemental material). Thus, *GIG2* is induced upon phagocytosis along with other GlcNAc catabolic genes, such as *NGT1* (13).

The *gig2* mutant showed decreased virulence. We investigated the impact of *GIG2* deletion during mammalian infection by using the mouse model of hematogenously disseminated candidiasis. When the homozygous mutant was used, none of the mice died until day 9, and almost 85% of the mice were alive at the end of day 11—the time by which all the mice infected with the wild type *C. albicans* strain had died. The virulence of the revertant was less than that of the wild-type strain, and 25% of the mice were alive at the end of day 11 (Fig. 3A).

Since kidneys are considered to be the organs preferentially

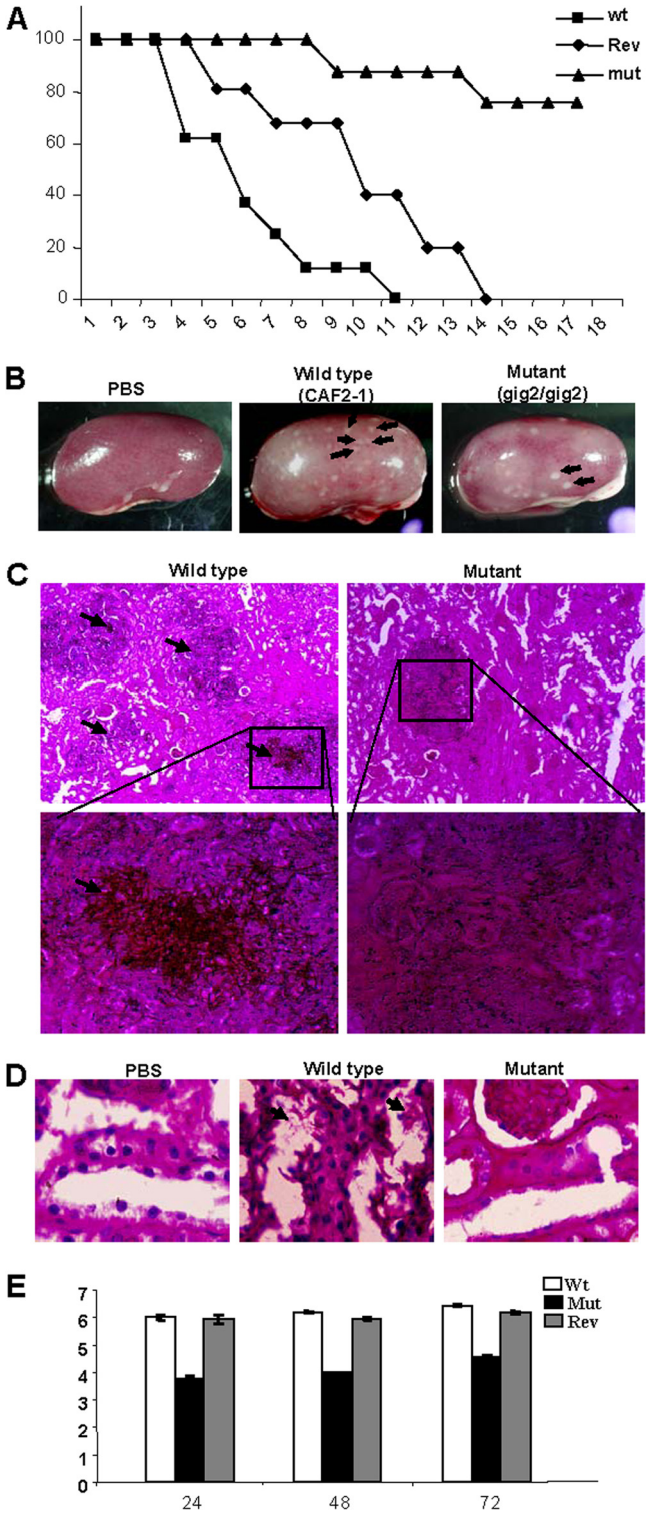

FIG 3 *GIG2* deficiency results in decreased virulence. (A) Infection of mice with the *gig2* mutant leads to enhanced survival. Mice were infected intravenously with 3×10^6 cells of the WT (CAF2-1), mutant, or revertant strain. The experiment was performed with 6 mice and was repeated three times. The percentage of mice surviving is given along the *y* axis, and the number of days after infection is given along the *x* axis. (B) Kidney surface views showing the severity of abscess formation. Abscesses (white pustules, indicated by black arrows) are more numerous in kidneys infected with the wild type (CAF2-1) than in *gig2* mutant-infected kidneys. (C) Periodic acid-Schiff staining of kidney sections from mice infected with the wild type or the *gig2* mutant 3 days after intravenous injection. As a control, mice were injected with PBS. Pictures were taken at magnifications of ×20 (top) and ×40 (bottom). The lower panels show magnifications of the boxed areas in the upper panels. Arrows point to filaments within the tissue. (D) Tubular casts and sloughing of the tubular cells, indicated by arrows. In mice given the mutant strain or PBS, the tubular space was almost clean. The experiments were performed in triplicate. (E) Subgroups of 3 to 5 mice were sacrificed at 24, 48, or 72 h after infection. The quantitative fungal burden in the kidney was measured by serial dilution and is expressed as log CFU per gram of tissue (*y* axis). Data in panels A and E are presented as means ± standard errors of the means from three separate experiments (P, <0.01).

colonized by *C. albicans*, one kidney from each mouse (5 mice/strain) was recovered 3 days postinfection and was preserved for histopathological studies. Before fixation, the entire surface of the kidney was photographed in order to determine the severity of lesion/abscess formation with each strain. A kidney from a PBS-injected mouse was used as a control. Numerous fungal abscesses were found with wild-type *C. albicans*, much fewer with the homozygous mutant, and none for PBS-injected mice (Fig. 3B). Histological sections of kidney recovered from wild-type-infected mice and stained with periodic acid–Schiff stain revealed huge and numerous focal collections of *Candida* filaments, whereas sections from the mutant showed very few areas of infection (Fig. 3C). The kidney sections of wild-type-infected mice also showed damage to almost the entire cortical region due to large necrotic areas and the sloughing of tubular epithelial cells into the lumen. With the mutant strain, the tubular space was almost free of such depositions (Fig. 3D). These observations also suggest that the severity of organ damage by the pathogen was reduced in the *gig2* mutant.

To evaluate whether the reduced virulence of the *gig2* strain was due to its reduced multiplication *in vivo*, we conducted a parallel set of experiments in which mice infected with either the WT or the mutant were sacrificed, and the level of fungal colonization of the kidney, one of the major target organs in systemic candidiasis, was determined. High fungal burdens were observed in WT-infected mice from 24 h to 72 h after the initiation of infection. CFU counts from the kidneys of mice infected with the *gig2* strain were significantly lower than those for WT-infected mice (Fig. 3E).

Identification of Gig2-interacting metabolites. To identify small metabolites bound to Gig2 protein, we used affinity protein purification coupled with mass spectrometry (27). Then bound metabolites were extracted in methanol from a purified protein-metabolite complex (Fig. 4A), and protein purity was examined using SDS gel electrophoresis after metabolite extraction (Fig. 4B). *N*-Glycolylneuraminate was identified as the metabolite interacting with Gig2 (Fig. 4C and D). However, *N*-glycolylneuraminate does not occur in *Candida albicans* (34). Hence, we concluded that the compound would be *N*-acetylneuraminate that had undergone oxidation during experimental procedures to yield *N*-glycolylneuraminate.

NMR analysis. Solution-state NMR spectroscopy was used to trace the catabolic route of *N*-acetylglucosamine-6-phosphate when the normal catabolic pathway is blocked, as in the case of the deacetylase (*dac1*) mutant. For this purpose, the three strains of *C. albicans* (the wild type and the *dac1* and *gig2* mutants) were grown in the presence of 1-^{13}C-labeled *N*-acetyl-D-glucosamine and/or glycerol. Glycerol was added to act as a carbon source, since the

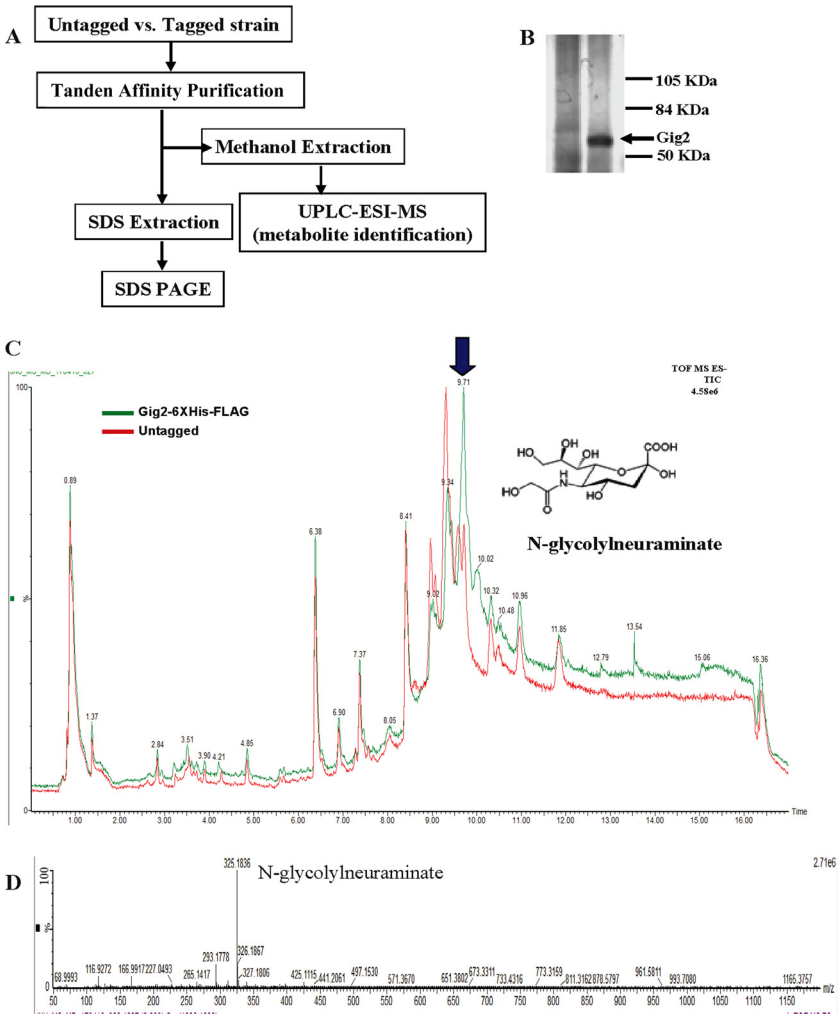

FIG 4 Identification of small metabolites associated with Gig2 protein. (A) Chart demonstrating the work flow for the identification of the metabolite bound to protein. (B) After two rounds of purification and extraction in methanol, the beads were boiled and were resolved on SDS-PAGE to check for the presence of purified Gig2. (C) LC plots of the small metabolites extracted from a protein (Gig2) (green) and the negative control (untagged) (red). Peak intensity is plotted against the retention times (in minutes) of corresponding mass spectra. All traces were smoothed by the Savitzky-Golay method using two passes with a window size of three scans. (D) Combined average mass spectra of the 9.02- to 10.020-min region. The mass of the Gig2-bound small metabolite is given along with its chemical identity. The peak mass (in atomic mass units) is shown along the *x* axis and the peak intensity (expressed as a percentage) along the *y* axis.

deacetylase mutant would be unable to utilize GlcNAc. The aqueous extract of the lysed culture was subjected to solution-state NMR spectroscopy. In the 2D $^{13}C,^{1}H$ HSQC spectrum of the aqueous extract of the *dac1* culture, we observed very strong resonance signals of 10-^{13}C-labeled *N*-acetyl-D-glucosamine-6-phosphate, 2-^{13}C-labeled *N*-acetyl-D-glucosamine-1-phosphate, and 1-^{13}C-labeled UDP-*N*-acetyl-D-glucosamine in addition to both α and β anomers of [1-^{13}C]GlcNAc (Fig. 5A). The ^{13}C labeling of the C-10, C-2, and C-1 carbons of GlcNAc-6-phosphate, GlcNAc-1-phosphate, and UDP-GlcNAc, respectively, confirms the pathway bifurcation once GlcNAc-6-PO_4 is unable to be catabolized further. Due to the high sensitivity of the cryoprobe, we also observed the weak resonance peaks of other carbons at their natural ^{13}C abundances in the 2D $^{13}C,^{1}H$ HSQC spectrum (Fig. 5B). Interestingly, we also observed a very weak resonance of 2-^{13}C-labeled *N*-acetylneuraminic acid (Fig. 5B). From the spectrum, it is very clear that the concentration of *N*-acetylneuraminic acid is much (>100-fold) lower than those of other metabolites, such as GlcNAc-6-phosphate, GlcNAc-1-phosphate, and UDP-GlcNAc. This confirms that the *dac1* mutant predominantly uses the pathway that leads to the formation of UDP-GlcNAc and also enters the *N*-acetylneuraminic acid metabolic pathway, albeit at a low rate.

A spectral comparison of the WT and the *gig2* mutant (Fig. 5C) showed that 1-^{13}C-labeled *N*-acetyl-D-glucosamine is completely catabolized in both strains and is used as a carbon source. A striking observation was that no resonance of *N*-acetylneuraminic acid could be found in the *gig2* mutant.

DISCUSSION

A member of the DUF1479 family of proteins. The unexplored sectors of the protein universe appear to have been shaped primarily by extreme diversification of known protein families, which then enabled organisms to evolve new functions and adapt to particular niches and habitats. Such unexplored proteins are often described as "hypothetical" but are bona fide proteins that have

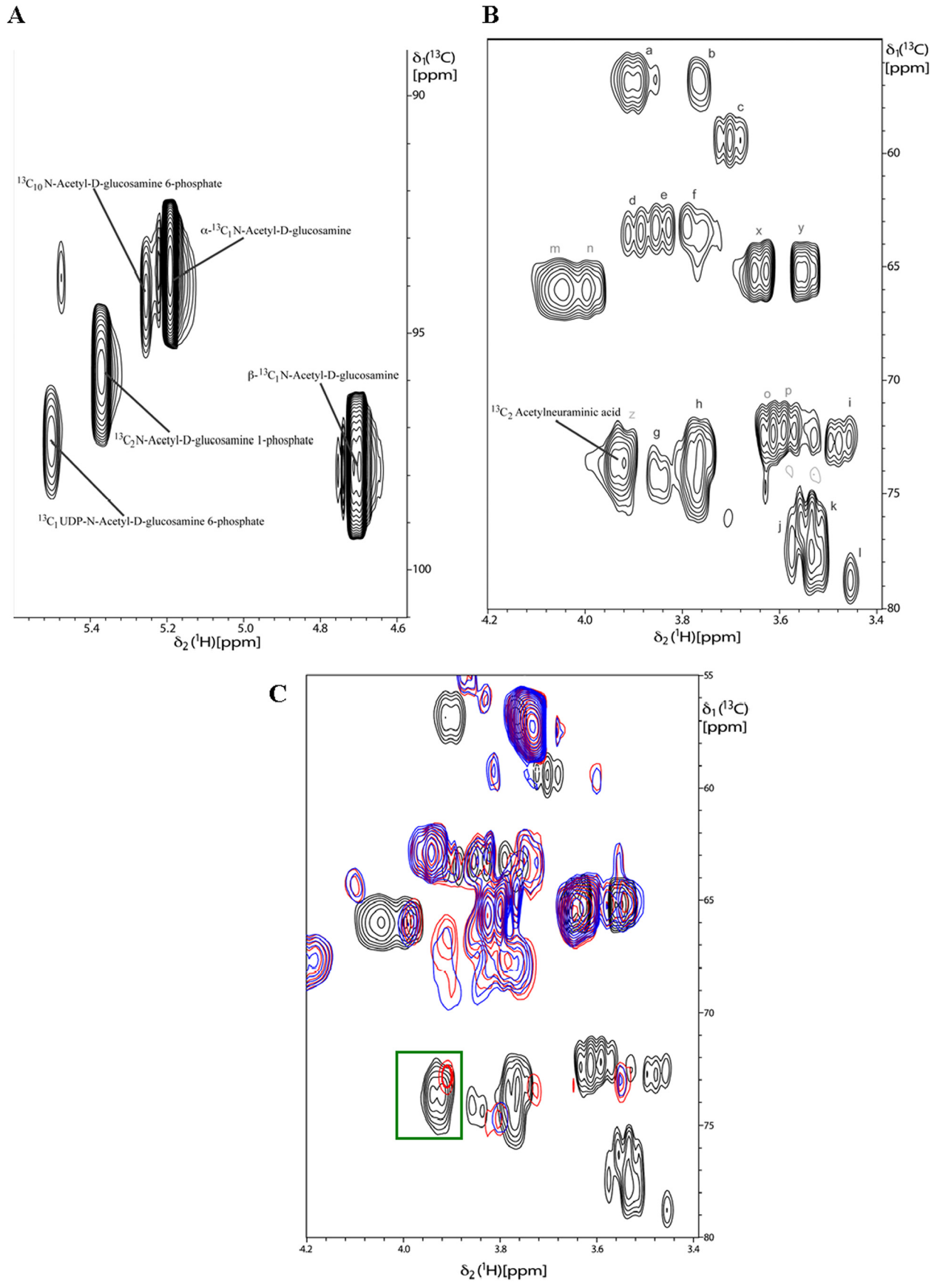

not yet been the focus of any detailed study. The PFAM database currently contains more than 2,200 such families, referred to as domains of unknown function (DUF) (35). ORF19.4783 was one such protein that showed the highest upregulation immediately after the set of GlcNAc catabolic genes. Like another novel GlcNAc-induced gene, *GIG1*, recently described by Gunasekera et al. (2010) (31), *GIG2* also resides on chromosome 1 and is not linked to the cluster of GlcNAc catabolic genes (*HXK1*, *NAG1*, and *DAC1*) on chromosome 6 or to the GlcNAc transporter *NGT1* on chromosome 3. Further, its mode of regulation also seems to be different from those of GlcNAc catabolic genes, such as *NGT1*, *HXK1*, *NAG1*, and *DAC1*, that are directly induced by GlcNAc. *GIG2*, in contrast, is induced in response to the GlcNAc catabolic intermediate GlcNAc-6-PO_4. This is clear from real-time RT-PCR analysis (Fig. 1D) and is supported by data from comparative expression profiles of some GlcNAc-inducible genes (see Fig. S2 in the supplemental material), showing the downregulation of a few genes, such as Orf19.4737 (*DHA12*) and Orf19.3392, along with *GIG2*, in the *hxk1* mutant in response to GlcNAc relative to expression in the wild type.

Gig2 is a member of the DUF1479 family in *C. albicans*, which shares its closest homology with a member of the enterobacteria (Protein Data Bank [PDB] identification [ID] code 2CSG). Jaroszewski et al. (2009) (35), in their *in silico* analysis based on remote homology, predicted that Gig2 was a putative oxidoreductase. A BLAST search (36) with *C. albicans* Gig2 revealed the conservation of this protein among various metazoans, plant, some fungal pathogens, and members of the *Enterobacteriaceae*, but it was absent in humans (see Fig. S4 in the supplemental material). The occurrence of Gig2 could not always be correlated with the occurrence of the GlcNAc catabolic genes. Probably, the presence of Gig2 homologues provides a competitive advantage for fungal pathogens and enterobacteria, enabling them to survive under niche-specific conditions, and contributes to their pathogenicity. Its occurrence in plants and metazoans could serve other, yet to be discovered purposes.

A novel pathway associated with *N*-acetylglucosamine metabolism in *Candida albicans*. Our qRT-PCR analysis for the relative expression of *GIG2* in *hxk1*, *dac1*, and *nag1* mutants indicated that Gig2 acts on a pathway downstream of the formation of GlcNAc-6-phosphate and branching at a point before the action of the deacetylase and deaminase genes of the GlcNAc catabolic pathway. Although reports on the formation of UDP-GlcNAc from GlcNAc-6-phosphate in *C. albicans* are available, nothing is known about the probable pathway that governs the formation of NANA (*N*-acetylneuraminic acid) from GlcNAc-6-phosphate. The occurrence of NANA has been reported in many cases and has been shown to modulate cell interactions and carbohydrate-dependent physiological or pathophysiological responses (37). Therefore, in a glucose-poor environment, where GlcNAc could predominate as a carbon source, GlcNAc-6-phosphate could be converted to NANA via a route that has been reported in humans.

NMR spectroscopy data with a GlcNAc-6-phosphate deacetylase mutant (where GlcNAc-6-phosphate could no longer be deacetylated and deamidated to be fed into the glycolytic pathway) showed a great preponderance of three molecules: GlcNAc 6-phosphate, GlcNAc-1-phosphate, and UDP-GlcNAc (Fig. 5A). All three of these molecules fall in the more thermodynamically favored first route (GlcNAc-6-phosphate → GlcNAc-1-phosphate → UDP-GlcNAc) of GlcNAc-6-phosphate catabolism once the normal glycolytic entry is blocked. *N*-Acetylneuraminic acid, a form of sialic acid, was also detected, albeit at low levels (Fig. 5B). Our data with the *gig2* mutant grown in the presence of nikkomycin Z (which acts on chitin synthase and competes for UDP-GlcNAc) showed no difference from wild-type cells. Had Gig2 been involved anywhere in this route of UDP-GlcNAc formation, a mutation in this gene would have affected this route, with obvious growth defects in the presence of nikkomycin Z. Under such circumstances, we presumed that Gig2 could be involved somewhere in the second route, probably emanating from GlcNAc-6-phosphate, that ultimately leads to the formation of NANA. The absence of an *N*-acetylneuraminic acid spectrum in NMR conducted with the *gig2* mutant lent credence to this hypothesis (Fig. 5C). Affinity purification coupled to mass spectrometric analysis for the study of the protein-metabolite interaction yielded *N*-glycolylneuraminic acid, which is an oxidized form of *N*-acetylneuraminic acid. We concluded that this molecule, in fact, could be *N*-acetylneuraminic acid, which during ESI or other experimental procedures probably underwent oxidation to yield *N*-glycolylneuraminic acid. This result strengthened our earlier presumption that Gig2 probably works in the route that ultimately leads to the metabolism of *N*-acetylneuraminic acid via GlcNAc-6-phosphate.

In humans, the pathways leading to the synthesis of *N*-acetylneuraminic acid (sialic acid) have been characterized. The first committed intermediate in the biosynthesis of sialic acid is *N*-acetylmannosamine (ManNAc), which is phosphorylated by ManNAc-6-kinase (38, 39) to initiate sialic acid biosynthesis in the cytosol. In principle, *N*-acetylmannosamine can be produced in the cell through one of two possible routes: (i) by UDP-*N*-acetylglucosamine (UDP-GlcNAc) 2-epimerase, which catalyzes the conversion of UDP-GlcNAc to ManNAc, or (ii) by GlcNAc-2-epimerase, which can produce ManNAc by catalyzing the reversible epimerization of GlcNAc to ManNAc. Studies suggest that the formation of ManNAc via the second route is negligible under physiological conditions, since GlcNAc is thermodynamically favored with an equilibrium ratio of almost 4:1. Thus, GlcNAc-2-epimerase has been postulated to divert ManNAc away

FIG 5 NMR analysis of pooled metabolites in the *dac1* mutant. (A) Selected regions of a 2D $^{13}C,^{1}H$ HSQC spectrum of an aqueous extract of the *dac1* mutant showing strong resonance peaks of 10-^{13}C-labeled *N*-acetyl-D-glucosamine-6-phosphate, 2-^{13}C-labeled *N*-acetyl-D-glucosamine-1-phosphate, and 1-^{13}C-labeled UDP-*N*-acetyl-D-glucosamine, in addition to both α and β anomers of 1-^{13}C-labeled *N*-acetyl-D-glucosamine. (B) Weak resonance signals of other carbons of GlcNAc (peaks a to l), GlcNAc-6-phosphate (peaks a to c, h, j, k, m to p, and z), and GlcNAc-1-phosphate (peaks a, d to f, h to i, and z) at the natural abundance of ^{13}C. The resonance peak of 2-^{13}C-labeled *N*-acetylneuraminic acid is marked. Peaks x and y could not be identified. The spectrum was acquired at 25°C on aqueous extracts with 8 scans per t_1 increment in the ^{13}C dimension on a 500-MHz NMR spectrometer equipped with a cryogenic 5-mm TCI probe head. Acquisition times for the ^{13}C and ^{1}H dimensions were 2.5 ms (t_{1max}) and 146.2 ms (t_{2max}), respectively. Spectral widths for the ^{13}C and ^{1}H dimensions were 25,155.08 Hz and 7,002.8 Hz, respectively. (C) Overlapped selected regions of 2D $^{13}C,^{1}H$ HSQC spectra of aqueous extracts of the wild type (red) and the *gig2* (blue) and *dac1* (black) mutants. The resonance signal of 2-^{13}C-labeled *N*-acetylneuraminic acid is boxed in green. 2-^{13}C-labeled *N*-acetylneuraminic acid is not found in the *gig2* mutant.

from sialic acid biosynthesis and into other glycolytic pathways (40). But under conditions of stress, such as those encountered when a pathogen evades host immune responses to establish infection, this equilibrium ratio might be altered so that the production of NANA is favored over that of GlcNAc-6-phosphate/UDP-GlcNAc. This hypothesis seems rational when one considers the importance of surface molecules of fungal cells *in vivo*. Future work aimed at delineating the exact reaction that Gig2 catalyzes, along with the metabolic profiling of the subsidiary pathways branching from GlcNAc-6-phosphate, would improve our understanding of the importance of intermediate products of GlcNAc metabolism.

ACKNOWLEDGMENTS

We thank Cheryl Gale, Masakazu Niimi, Janet Quinn, James B. Konopka, A. D. Johnson, and Alistair J. P. Brown for generously providing the plasmids and *C. albicans* strains used in this study. We also thank A. K. Dinda, AIIMS, New Delhi, India, for his kind help in performing histopathological studies. P. M. N. Rajesh, Waters India Pvt. Ltd., Bangalore, India, helped with the UPLC-coupled MS analysis. The Confocal Microscope Facility at NIPGR is acknowledged for the confocal data.

We thank the Department of Biotechnology (DBT), Government of India, for providing financial support toward the procurement of 500-MHz and 700-MHz NMR spectrometers at the ICGEB and NII, New Delhi, India. S.G. and K.H.R. are recipients of a CSIR-SRA fellowship.

REFERENCES

1. **Odds FC.** 1988. *Candida* and candidosis. Bailliere Tindall, London, United Kingdom.
2. **Perlroth J, Choi B, Spellberg B.** 2007. Nosocomial fungal infections: epidemiology, diagnosis, and treatment. Med. Mycol. **45:**321–346. http://dx.doi.org/10.1080/13693780701218689.
3. **Calderone RA, Clancy CJ.** 2012. *Candida* and candidiasis, 2nd ed. ASM Press, Washington, DC.
4. **Ene IV, Adya AK, Wehmeier S, Brand AC, MacCallum DM, Gow NA, Brown AJ.** 2012. Host carbon sources modulate cell wall architecture, drug resistance and virulence in a fungal pathogen. Cell. Microbiol. **14:**1319–1335. http://dx.doi.org/10.1111/j.1462-5822.2012.01813.x.
5. **Ene IV, Cheng SC, Netea MG, Brown AJ.** 2013. Growth of *Candida albicans* cells on the physiologically relevant carbon source lactate affects their recognition and phagocytosis by immune cells. Infect. Immun. **81:**238–248. http://dx.doi.org/10.1128/IAI.01092-12.
6. **Simonetti N, Strippoli V, Cassone A.** 1974. Yeast-mycelial conversion induced by *N*-acetyl-D-glucosamine in *Candida albicans*. Nature **250:**344–346. http://dx.doi.org/10.1038/250344a0.
7. **Natarajan K, Rai YP, Datta A.** 1984. Induction of *N*-acetyl-D-glucosamine catabolic enzymes and germinative response in *Candida albicans*. Biochem. Int. **9:**735–744.
8. **Huang G, Yi S, Sahni N, Daniels KJ, Srikantha T, Soll DR.** 2010. *N*-Acetylglucosamine induces white to opaque switching, a mating prerequisite in *Candida albicans*. PLoS Pathog. **6:**e1000806. http://dx.doi.org/10.1371/journal.ppat.1000806.
9. **Milewski S, Gabriel I, Olchowy J.** 2006. Enzymes of UDP-GlcNAc biosynthesis in yeast. Yeast **23:**1–14. http://dx.doi.org/10.1002/yea.1337.
10. **Kumar MJ, Jamaluddin MS, Natarajan K, Kaur D, Datta A.** 2000. The inducible *N*-acetylglucosamine catabolic pathway gene cluster in *Candida albicans*: discrete *N*-acetylglucosamine-inducible factors interact at the promoter of *NAG1*. Proc. Natl. Acad. Sci. U. S. A. **97:**14218–14223. http://dx.doi.org/10.1073/pnas.250452997.
11. **Singh P, Ghosh S, Datta A.** 2001. Attenuation of virulence and changes in morphology in *Candida albicans* by disruption of the *N*-acetylglucosamine catabolic pathway. Infect. Immun. **69:**7898–7903. http://dx.doi.org/10.1128/IAI.69.12.7898-7903.2001.
12. **Yamada-Okabe T, Sakamori Y, Mio T, Yamada-Okabe H.** 2001. Identification and characterization of the genes for *N*-acetylglucosamine kinase and *N*-acetylglucosamine phosphate deacetylase in the pathogenic fungus *Candida albicans*. Eur. J. Biochem. **268:**2498–2505. http://dx.doi.org/10.1046/j.1432-1327.2001.02135.x.
13. **Alvarez FJ, Konopka JB.** 2007. Identification of an *N*-acetylglucosamine transporter that mediates hyphal induction in *Candida albicans*. Mol. Biol. Cell **18:**965–975. http://dx.doi.org/10.1091/mbc.E06-10-0931.
14. **Naseem S, Gunasekera A, Araya E, Konopka JB.** 2011. *N*-Acetylglucosamine (GlcNAc) induction of hyphal morphogenesis and transcriptional responses in *Candida albicans* are not dependent on its metabolism. J. Biol. Chem. **286:**28671–28680. http://dx.doi.org/10.1074/jbc.M111.249854.
15. **Boehmelt G, Wakeham A, Elia A, Sasaki T, Plyte S, Potter J, Yang Y, Tsang E, Ruland J, Iscove NN, Dennis JW, Mak TW.** 2000. Decreased UDP-GlcNAc levels abrogate proliferation control in EMeg32 deficient cells. EMBO. J. **19:**5092–5104. http://dx.doi.org/10.1093/emboj/19.19.5092.
16. **Guthrie C, Fink GR.** 1991. Guide to yeast genetics and molecular biology. Academic Press, San Diego, CA.
17. **Fonzi A, Irwin MY.** 1993. Isogenic strain construction and gene mapping in *Candida albicans*. Genetics **134:**717–728.
18. **Shepherd MG, Yin CY, Ram SP, Sullivan PA.** 1980. Germ tube induction in *Candida albicans*. Can. J. Microbiol. **26:**21–26. http://dx.doi.org/10.1139/m80-004.
19. **Geitz RD, Woods RA.** 1998. Transformation of yeast by the lithium acetate/single-stranded carrier DNA/PEG method. Methods Microbiol. **26:**53–66. http://dx.doi.org/10.1016/S0580-9517(08)70325-8.
20. **Noble SM, Johnson AD.** 2005. Strains and strategies for large scale gene deletion studies of the diploid human fungal pathogen *Candida albicans*. Eukaryot. Cell **4:**298–309. http://dx.doi.org/10.1128/EC.4.2.298-309.2005.
21. **Gerami-Nejad M, Berman J, Gale CA.** 2001. Cassettes for PCR-mediated construction of green, yellow, and cyan fluorescent protein fusions in *Candida albicans*. Yeast **18:**859–864. http://dx.doi.org/10.1002/yea.738.
22. **Longtine MS, McKenzie A, III, Demarini DJ, Shah NG, Wach A, Brachat A, Philippsen P, Pringle JR.** 1998. Additional modules for versatile and economical PCR-based gene deletion and modification in *Saccharomyces cerevisiae*. Yeast **14:**953–961.
23. **Kaneko A, Umeyama T, Hanaoka N, Monk BC, Uehara Y, Niimi M.** 2004. Tandem affinity purification of the *Candida albicans* septin protein complex. Yeast **21:**1025–1033. http://dx.doi.org/10.1002/yea.1147.
24. **Smith DA, Nicholls S, Morgan BA, Brown AJ, Quinn J.** 2004. A conserved stress-activated protein kinase regulates a core stress response in the human pathogen *Candida albicans*. Mol. Biol. Cell **15:**4179–4190. http://dx.doi.org/10.1091/mbc.E04-03-0181.
25. **Schmittgen TD, Livak KJ.** 2008. Analyzing real-time PCR data by the comparative C_T method. Nat. Protoc. **3:**1101–1108. http://dx.doi.org/10.1038/nprot.2008.73.
26. **Rao KH, Ghosh S, Natarajan K, Datta A.** 2013. *N*-Acetylglucosamine kinase, HXK1 is involved in morphogenetic transition and metabolic gene expression in *Candida albicans*. PLoS One **8:**e53638. http://dx.doi.org/10.1371/journal.pone.0053638.
27. **Li X, Gianoulis TA, Yip KY, Gerstein M, Snyder M.** 2010. Extensive *in vivo* metabolite-protein interactions revealed by large scale systematic analyses. Cell **143:**639–650. http://dx.doi.org/10.1016/j.cell.2010.09.048.
28. **Yu SL, An YJ, Yang HJ, Kang MS, Kim HY, Wen H, Jin X, Kwon HN, Min KJ, Lee SK, Park S.** 2013. Alanine-metabolizing enzyme Alt1 is critical in determining yeast life span, as revealed by combined metabolomic and genetic studies. J. Proteome Res. **12:**1619–1627. http://dx.doi.org/10.1021/pr300979r.
29. **Findeisen M, Brand T, Berger S.** 2007. A ^{1}H NMR thermometer suitable for cryoprobes. Magn. Reson. Chem. **45:**175–178. http://dx.doi.org/10.1002/mrc.1941.
30. **Keller R.** 2004. The computer aided resonance assignment tutorial, 1st ed. Cantina Verlag, Goldau, Switzerland.
31. **Gunasekera A, Alvarez FJ, Douglas LM, Wang HX, Rosebrock AP, Konopka JB.** 2010. Identification of *GIG1*, a GlcNAc-induced gene in *Candida albicans* needed for normal sensitivity to the chitin synthase inhibitor nikkomycin Z. Eukaryot. Cell **9:**1476–1483. http://dx.doi.org/10.1128/EC.00178-10.
32. **Braun BR, Head WS, Wang MX, Johnson AD.** 2000. Identification and characterization of *TUP1*-regulated genes in *Candida albicans*. Genetics **156:**31–44. http://www.genetics.org/content/156/1/31.long.
33. **Lorenz MC, Bender JA, Fink GR.** 2004. Transcriptional response of *Candida albicans* upon internalization by macrophages. Eukaryot. Cell **3:**1076–1087. http://dx.doi.org/10.1128/EC.3.5.1076-1087.2004.
34. **Soares RMA, Soares RMDA, Alviano DS, Angluster J, Alviano CS, Travassos LR.** 2000. Identification of sialic acids on the cell surface of

Candida albicans. Biochim. Biophys. Acta **1474:**262–268. http://dx.doi.org/10.1016/S0304-4165(00)00003-9.
35. **Jaroszewski L, Li Z, Krishna SS, Bakolitsa C, Wooley J, Deacon AM, Wilson IA, Godzik A.** 2009. Exploration of uncharted regions of the protein universe. PLoS Biol. **7:**e1000205. http://dx.doi.org/10.1371/journal.pbio.1000205.
36. **Altschul SF, Gish W, Miller W, Myers EW, Lipman DJ.** 1990. Basic local alignment search tool. J. Mol. Biol. **215:**403–410. http://dx.doi.org/10.1016/S0022-2836(05)80360-2.
37. **Alviano CS, Travassos LR, Schauer R.** 1999. Sialic acids in fungi: a minireview. Glycoconj. J. **16:**545–554. http://dx.doi.org/10.1023/A:1007078106280.
38. **Stäsche R, Hinderlich S, Weise C, Effertz K, Lucka L, Moormann P, Reutter W.** 1997. A bifunctional enzyme catalyzes the first two steps in *N*-acetylneuraminic acid biosynthesis of rat liver. Molecular cloning and functional expression of UDP-*N*-acetyl-glucosamine 2-epimerase/*N*-acetylmannosamine kinase. J. Biol. Chem. **272:**24319–24324.
39. **Lucka L, Krause M, Danker K, Reutter W, Horstkorte R.** 1999. Primary structure and expression analysis of human UDP-*N*-acetylglucosamine-2-epimerase/*N*-acetylmannosamine kinase, the bifunctional enzyme in neuraminic acid biosynthesis. FEBS Lett. **454:**341–344. http://dx.doi.org/10.1016/S0014-5793(99)00837-6.
40. **Luchansky SJ, Yarema KJ, Takahashi S, Bertozzi CR.** 2003. GlcNAc 2-epimerase can serve a catabolic role in sialic acid metabolism. J. Biol. Chem. **278:**8035–8042. http://dx.doi.org/10.1074/jbc.M212127200.